



# Circadian Rhythms and Sleep Are Dependent Upon Expression Levels of Key Ubiquitin Ligase *Ube3a*

Shu-qun Shi<sup>1†</sup>, Carrie E. Mahoney<sup>2†</sup>, Pavel Houdek<sup>3</sup>, Wenling Zhao<sup>2</sup>, Matthew P. Anderson<sup>2,4</sup>, Xinming Zhuo<sup>5</sup>, Arthur Beaudet<sup>6</sup>, Alena Sumova<sup>3</sup>, Thomas E. Scammell<sup>2</sup> and Carl Hirschie Johnson<sup>1\*</sup>

<sup>1</sup> Department of Biological Sciences, Vanderbilt University, Nashville, TN, United States, <sup>2</sup> Department of Neurology, Beth Israel Deaconess Medical Center, Boston, MA, United States, <sup>3</sup> Laboratory of Biological Rhythms, Institute of Physiology of the Czech Academy of Sciences, Prague, Czechia, <sup>4</sup> Department of Pathology, Beth Israel Deaconess Medical Center, Harvard Medical School, Boston, MA, United States, <sup>5</sup> Department of Molecular and Human Genetics, Baylor College of Medicine, Houston, TX, United States, <sup>6</sup> Luna Genetics, Inc., Houston, TX, United States

## OPEN ACCESS

### Edited by:

Emi Hasegawa,  
University of Tsukuba, Japan

### Reviewed by:

Li Wang,  
Children's National Hospital,  
United States  
Ling Shan,  
Netherlands Institute for Neuroscience  
(KNAW), Netherlands

### \*Correspondence:

Carl Hirschie Johnson  
carl.h.johnson@vanderbilt.edu

† These authors share first authorship

### Specialty section:

This article was submitted to  
Individual and Social Behaviors,  
a section of the journal  
Frontiers in Behavioral Neuroscience

Received: 16 December 2021

Accepted: 09 February 2022

Published: 23 March 2022

### Citation:

Shi S-q, Mahoney CE, Houdek P, Zhao W, Anderson MP, Zhuo X, Beaudet A, Sumova A, Scammell TE and Johnson CH (2022) Circadian Rhythms and Sleep Are Dependent Upon Expression Levels of Key Ubiquitin Ligase *Ube3a*. *Front. Behav. Neurosci.* 16:837523. doi: 10.3389/fnbeh.2022.837523

Normal neurodevelopment requires precise expression of the key ubiquitin ligase gene *Ube3a*. Comparing newly generated mouse models for *Ube3a* downregulation (models of Angelman syndrome) vs. *Ube3a* upregulation (models for autism), we find reciprocal effects of *Ube3a* gene dosage on phenotypes associated with circadian rhythmicity, including the amount of locomotor activity. Consistent with results from neurons in general, we find that *Ube3a* is imprinted in neurons of the suprachiasmatic nuclei (SCN), the pacemaking circadian brain locus, despite other claims that SCN neurons were somehow exceptional to these imprinting rules. In addition, *Ube3a*-deficient mice lack the typical drop in wake late in the dark period and have blunted responses to sleep deprivation. Suppression of physical activity by light in *Ube3a*-deficient mice is not due to anxiety as measured by behavioral tests and stress hormones; quantification of stress hormones may provide a mechanistic link to sleep alteration and memory deficits caused by *Ube3a* deficiency, and serve as an easily measurable biomarker for evaluating potential therapeutic treatments for Angelman syndrome. We conclude that reduced *Ube3a* gene dosage affects not only neurodevelopment but also sleep patterns and circadian rhythms.

**Keywords:** circadian, sleep, ubiquitin ligase, neurodevelopmental disorders, Angelman syndrome, UBE3A (E6AP), imprinting, autism

## INTRODUCTION

Although single-gene neurological disorders are uncommon, they are extremely valuable for investigating genetic and pathological mechanisms because their genetic underpinnings are usually more straightforward than in more complex genetic disorders (Shi and Johnson, 2019). Among monogenic neurodevelopmental disorders, Angelman syndrome (AS) is particularly interesting;

**Abbreviations:** LD, light/dark cycle (LD 12:12 = 12-h light/12-h dark cycle); LL, constant light conditions; DD, constant darkness conditions; CT, circadian time, where CT0 is subjective dawn and CT12 is subjective dusk; ZT, phase/time in the LD cycle, where ZT0 is lights-on and ZT12 is lights-off in a LD 12:12 cycle.

deletion of only one copy (the maternal allele) of the ubiquitin ligase gene *Ube3a* confers haploinsufficiency because the paternal allele of *Ube3a* is imprinted and silenced in neurons of both AS and non-affected subjects (Jiang et al., 2010). This haploinsufficiency leads to AS, resulting in mental disability, with impaired speech, delayed development, sleep disorders, epilepsy, and motor difficulties (Robb et al., 1989; Laan et al., 1999; Williams et al., 2006). Interestingly, the paternal imprinting of *Ube3a* occurs only in neurons (Albrecht et al., 1997; Jiang et al., 1998; Weeber et al., 2003), and not in glia or non-neural peripheral tissues (Nakao et al., 1994; Dindot et al., 2008; Gustin et al., 2010; Judson et al., 2014). In healthy subjects, the maternal copy of *Ube3a* is active in adult neurons while the paternal copy is silenced. On the other hand, extra copies of *Ube3a*, as in duplications and triplications of the region of chromosome 15 that harbors *Ube3a* are a common large genetic alteration that is linked to autism spectrum disorder (ASD; Sutcliffe et al., 1997; Lehman, 2009). Therefore, appropriate gene dosage of *Ube3a* is critical for normal neural development—the equivalent of one active allele allows normal development, whereas too little leads to AS, and too much leads to autism.

About 50–75% of individuals with AS have a sleep disorder, such as short sleep duration and increased sleep onset latency, and these sleep disruptions are one of the syndrome's most stressful problems for families caring for a person with AS (Smith et al., 1996; Pelc et al., 2008; Goldman et al., 2012). These sleep phenotypes in AS could be due to a misalignment of the circadian system, as the timing of sleep is regulated by the circadian clock (Scammell et al., 2017; Schwartz and Klerman, 2019). While most research on sleep disruptions in AS is limited to clinical/behavioral observations, one study of daily profiles of the hormone melatonin concluded there was a high prevalence of circadian rhythm sleep disorders in AS (Takaesu et al., 2012).

Though clinical research on sleep in AS is limited, animal models provide many opportunities to identify the impact of *Ube3a* deficiency on the circadian and sleep systems. The two currently available mouse models for AS include an exon 5-specific deletion within *Ube3a* that also creates a frame shift (herein called Ud5-m-/p+ for deletion of exon 5 from the transcriptional start site in the maternal *Ube3a* allele combined with an intact paternal allele) (Jiang et al., 1998). The second model is caused by a larger (1.6 Mb) chromosomal deletion that removes the maternal copies of *Ube3a* as well as the adjacent *Atp10a* and *Gabrb3* genes (herein called UG-m-/p+) (Jiang et al., 2010). These mouse models demonstrate phenotypes similar to those seen in human AS patients, including motor dysfunction, impaired locomotion, seizures, learning deficits, abnormal EEG (electroencephalogram) patterns, and changes in CaMKII phosphorylation that reduce hippocampal long-term potentiation (LTP; Jiang et al., 1998; Weeber et al., 2003; Colas et al., 2005; van Woerden et al., 2007; Shi et al., 2015). Most people with AS (~75%) have large deletions of the maternal chr15q11-13 alleles, including *Ube3a*, *Atp10a*, and *Gabrb3*, and therefore the larger-deletion UG-m-/p+ mouse model is generally considered to better reflect AS in humans than the smaller U-m-/p+ deletion model (Jiang et al., 2010). On the other hand, the Ud5-m-/p+

model is specific for the *Ube3a* gene that is primarily responsible for AS and therefore allows precise association of aberrant phenotypes with reduced dosage of *Ube3a* (Jiang et al., 1998) (but see the paragraph below concerning inconsistencies with the Ud5-m-/p+ model).

We have reported that the robustness of circadian rhythms is diminished in both Ud5-m-/p+ and UG-m-/p+ mice as assessed by longer free-running periods in constant darkness (DD), accelerated phase resetting, and greater suppression of activity in constant light (LL; Shi et al., 2015). Another research group has reported that Ud5-m-/p+ mice have a reduced capacity to accumulate sleep pressure, both during their active period and in response to forced sleep deprivation (Ehlen et al., 2015). Contrary to predictions, they also reported that the neurons of the suprachiasmatic nuclei (SCN, the site of the master circadian clockwork in mammals) were unusual in that they expressed more UBE3A protein than expected, and therefore the paternal allele of *Ube3a* was exceptionally not imprinted in the central clock neurons of Ud5-m-/p+ mice (Ehlen et al., 2015; Jones et al., 2016). This observation was particularly surprising because the circadian period is lengthened in cultured SCN brain slices of Ud5-m-/p+ mice isolated *in vitro* (Shi et al., 2015) and that result is difficult to explain if UBE3A levels were unchanged.

Those disparate observations were made with the Ud5-m-/p+ mouse model (Ehlen et al., 2015; Shi et al., 2015; Jones et al., 2016), which has been the standard mouse model of AS. However, multiple labs have reported challenges with the Ud5-m-/p+ model such as strain dependency and loss of phenotype over time (Huang et al., 2013; Born et al., 2017; Dodge et al., 2020). Moreover, the Ud5-m-/p+ mouse model may not be a complete null mutation of *Ube3a* because the deleted exon 5 is subject to brain-specific alternative splicing that can result in a truncated *Ube3a* transcript (Dr. Scott Dindot, personal communication, September 2021). This truncated mRNA is not translated and its functions, if any, are unknown. These inconsistencies have led to the generation of new animal models for AS which could better reflect the human AS phenotype, including a model in rats (Dodge et al., 2020). To take full advantage of the genetics that mouse models enable, it is essential to develop a mouse line that specifically targets the *Ube3a* gene with a consistent phenotype similar to Angelman syndrome. Because a larger deletion within the *Ube3a* gene should more closely mimic the condition in people with AS, we studied the circadian and sleep phenotypes of a new mouse model, i.e., Ud6-m-/p+ mice that harbor a larger deletion of *Ube3a*'s exon 6 (a 1247 nt deletion that also confers a frame shift, whereas the deletion in exon 5 of the Ud5-m-/p+ mouse is only 290 nt, **Figure 1A**). We found that phenotypes of this new model recapitulate, confirm, and extend the observations previously made with the Ud5-m-/p+ model for circadian (Shi et al., 2015) and sleep behavior (Ehlen et al., 2015). Moreover, and in contrast to previous studies (Ehlen et al., 2015; Jones et al., 2016), we find that the expression of UBE3A in the SCN to a degree that is consistent with paternal imprinting, and therefore the neurons within the SCN are not an exception to the conclusion that the paternal allele of *Ube3a* is imprinted within neurons.

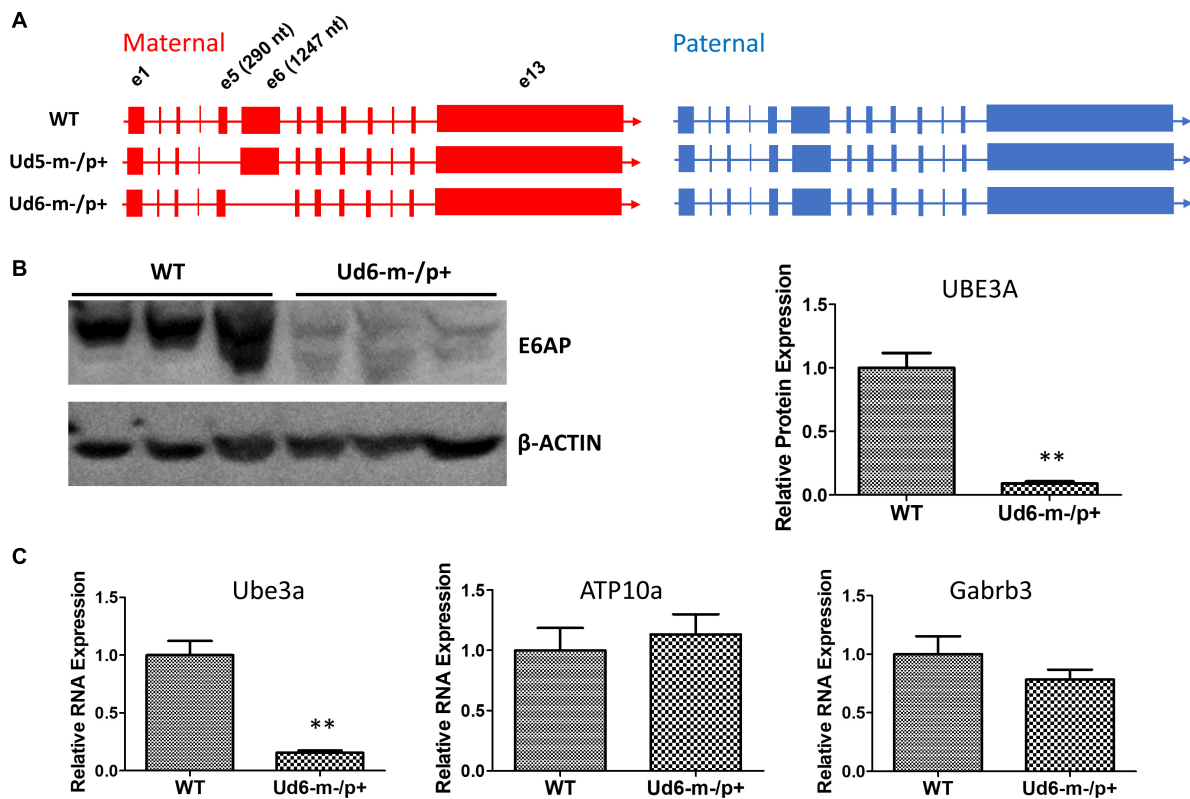


**FIGURE 1** | *Ube3a* is imprinted in the brain of the Ud6-m-/p+ mouse. **(A)** Female mice harboring one *Ube3a* knockout allele (left panel) were crossed with wild-type background (WT C57BL/6J) male mice (right panel) to obtain the maternal deletion Angelman model mice. The maternal and paternal *Ube3a* allele arrangements are WT (upper), the original Angelman model mouse strain harboring an exon 5 deletion in *Ube3a* gene, Ud5-m-/p+ (middle), and the new strain knockout of exon 6 in the *Ube3a* gene, Ud6-m-/p+ (lower). **(B)** Left panel, immunoblots for UBE3A protein in the cerebellum of Ud6-m-/p+ and WT mice.  $\beta$ -ACTIN serves as the loading control (each lane comes from a separate mouse; one representative immunoblot is shown). Right panel, densitometric analyses of the immunoblot (the expression of WT is normalized to 1.0,  $n = 3$  for both WT and Ud6-m-/p+). \*\* $p < 0.01$  by two-tail unpaired *T* test, error bars are SEM. **(C)** *Ube3a*, *ATP10a*, and *Gabrb3* mRNA transcript abundances in cerebellum of Ud6-m-/p+ and WT mice were quantified by real-time PCR ( $n = 3$  for both WT and Ud6-m-/p+). \*\* $p < 0.01$  by two-tail unpaired *T* test, error bars are SEM.

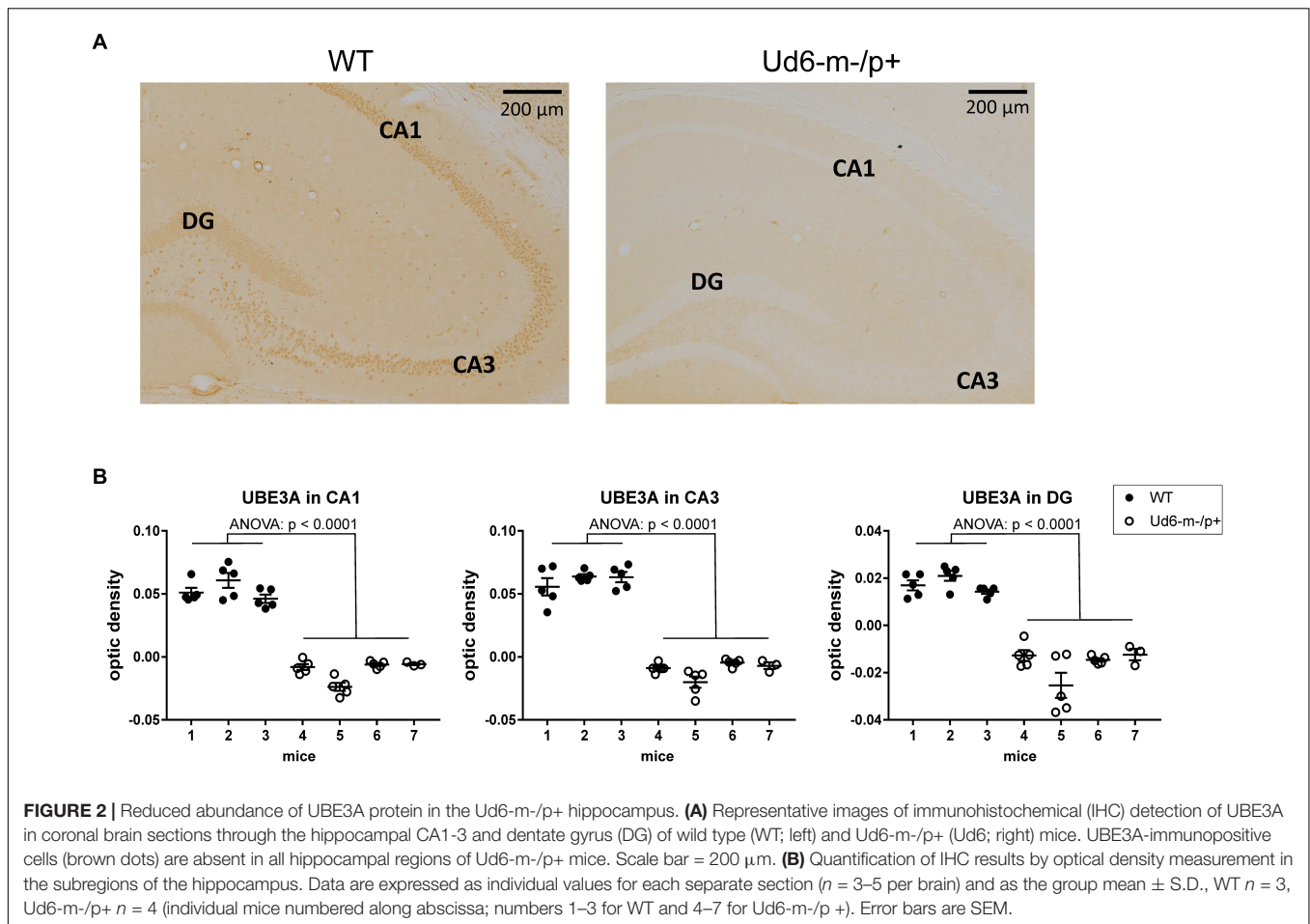
## RESULTS

### Reduction of UBE3A Expression in the Ud6-m-/p+ Brain

To confirm that the levels of UBE3A protein were downregulated by imprinting of the paternal allele in the Ud6-m-/p+ mouse, we measured UBE3A levels in the cerebellum of brains by immunoblotting with an anti-UBE3A antibody. In Ud6-m-/p+ mice, UBE3A protein was reduced to only 10% of the WT level (Figure 1B). Consistent with the lower gene expression indicated by minimal UBE3A protein levels, the *Ube3a* transcript abundance in the cerebellum of Ud6-m-/p+ mice was only 15% that of the WT levels. At the same time, mRNA levels for the *Atp10a* and *Gabrb3* genes did not differ between WT and Ud6-m-/p+ mice (Figure 1C). The *Atp10a* and *Gabrb3* genes are immediately adjacent to *Ube3a* on mouse chromosome 7 and are not imprinted; therefore, they serve as controls for the specificity of downregulation of *Ube3a* in the Ud6-m-/p+ mouse.

To explore and visualize the spatial expression of *Ube3a* expression in two key areas of the brain, we conducted

immunohistochemical (IHC) localization of UBE3A in the hippocampus and suprachiasmatic nuclei [SCN, the site of the central mammalian biological clock mechanism (Reppert and Weaver, 2002)]. We detected UBE3A immunopositivity by standard avidin-biotin methods, or by fluorescent dyes for antigen co-localization (Sumová et al., 2002; Liska et al., 2021). The IHC results were quantified by measuring optical density as a measure of the expressed protein levels in the hippocampal CA1, CA3, and DG regions, where the cells are in tight proximity (cell bodies are dense and difficult to reliably resolve), and by calculating the number of individual immunopositive cells in the SCN (cell number was used for the SCN because of its unique anatomy and structure that allows cells bodies to be resolved). The optical density of UBE3A staining was abundant in all three hippocampal regions of the WT mice, but it was below the detection limit in Ud6-m-/p+ mice (Figure 2A). UBE3A expression was consistently reduced across the entire hippocampus including the CA1, CA3, and DG regions (ANOVA,  $p < 0.0001$  for all regions, Figure 2B) that are important regions for functional learning and memory



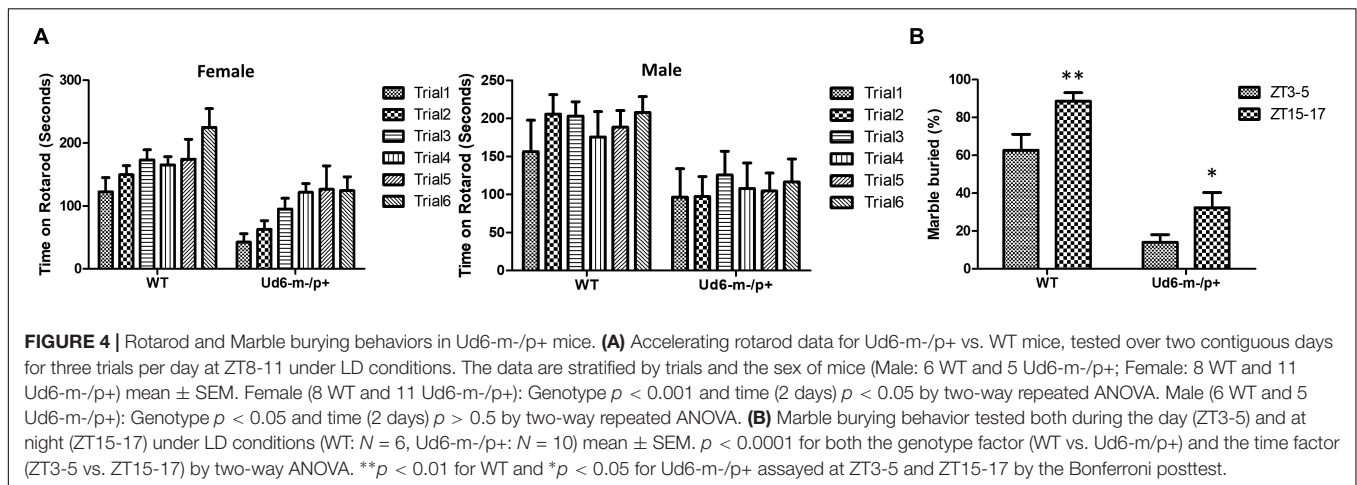
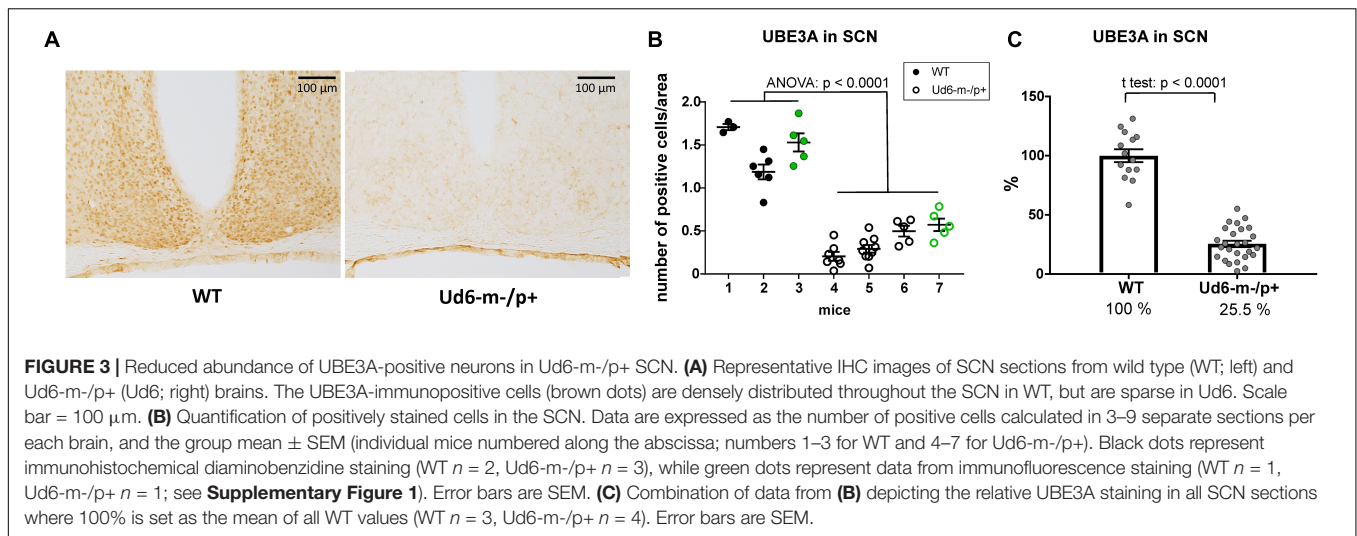
(Jiang et al., 1998; Dodge et al., 2020). Therefore, *Ube3a* protein expression was silenced in the hippocampus of *Ud6-m-/p+* mice.

Additionally, we found robust suppression of UBE3A-immunopositivity in the SCN of *Ud6-m-/p+* mice (Figure 3A). *Ud6-m-/p+* mice had only about 25% of the number of SCN cells expressing UBE3A (Figure 3B, ANOVA;  $p < 0.0001$ ) compared to the SCN in WT mice (Figure 3C, *t*-test;  $p < 0.0001$ ). By examination of confocal images under high magnification, we confirmed that *Ube3a* is expressed in neurons but not in astroglia within the SCN and hippocampus because UBE3A co-localized with ELAVL4, a marker for neurons (Jung and Lee, 2021), but not with GFAP, a marker for astrocytes (Brenner et al., 1994; Supplementary Figure 1). In contrast to a prior study of the *Ud5-m-/p+* mouse (Jones et al., 2016), we clearly confirm that UBE3A is downregulated in the SCN of *Ud6-m-/p+* mice to an extent that is entirely consistent with imprinting of the paternal *Ube3a* allele in SCN neurons. If the paternal allele of *Ube3a* were fully active, there should be 50% of UBE3A expression as compared with WT because of the deletion of the maternal allele; however, with our criterion that is based upon the number of UBE3A cells, we find that 25.5% of SCN cells retain some UBE3A expression (Figure 3C). Detailed inspection of the overlap between UBE3A and ELAVL4 or GFAP staining revealed that the majority of the UBE3A-positive cells were neurons but there were a few cells

in the SCN sections that expressed UBE3A but not ELAVL4 or GFAP (not shown). Therefore, some of these UBE3A-positive cells within the SCN of *Ud6-m-/p+* mice may be non-neuronal.

### Altered Rotarod and Marble-Burying Phenotypes in *Ud6-m-/p+* Mice

The previously generated mouse models of Angelman syndrome (*Ud5-m-/p+* and *UG-m-/p+*) exhibit altered phenotypes in rotarod and marble-burying behavioral tests (Jiang et al., 1998, 2010; Sonzogni et al., 2018). We used the accelerating rotarod to study motor coordination and motor learning skills and confirmed that the *Ud6-m-/p+* mice also performed significantly worse on the rotarod than their WT littermates ( $p < 0.001$  for females and  $p < 0.05$  for males for the genotype factor by two-way repeated ANOVA, Figure 4A). There was a clear sex difference in the improvement in fall-off time over the trial testing, with females exhibiting better motor learning over trials in the task than males (Figure 4A). AS model mice also have altered marble burying behavior, which is a test used to assess repetitive and perseverative behavior as well as anxiety (Sonzogni et al., 2018). We found that *Ud6-m-/p+* mice bury fewer marbles than WT mice when tested both in the day (ZT3-5) and at night (ZT15-17), indicating reduced anxiety and compulsiveness

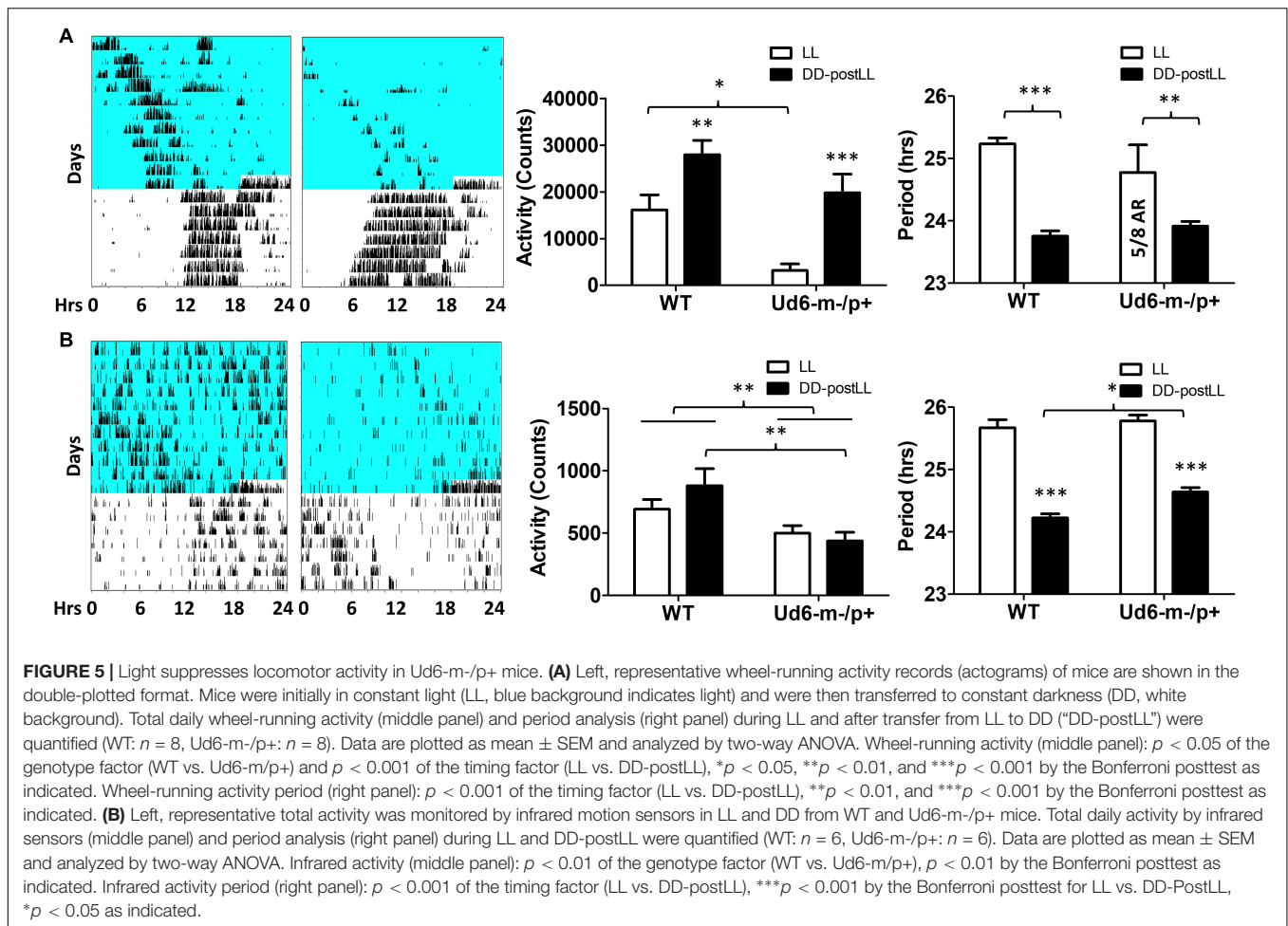


(Thomas et al., 2009; Angoa-Pérez et al., 2013;  $p < 0.0001$  for the genotype factor by two-way ANOVA, **Figure 4B**). We also confirmed that the repetitive and perseverative behavior as well as anxiety tested by marble burying has a significant day and night variation in WT animals ( $p = 0.004$  by  $T$  test, **Figure 4B**), suggesting an importance of circadian factor in preclinical study. Therefore, consistent with other studies, the Ud6-m-/p+ model mice exhibit altered behaviors as compared with WT littermates.

### Haploinsufficiency of *Ube3a* Alters Locomotor Activity Patterns in Response to LL

Environmental exposure to constant light (LL) disrupts and/or suppresses circadian activity patterns in mice, and we previously reported an enhanced effect of LL on Ud5-m-/p+ mice (Shi et al., 2015). We observed a similar LL-dependent effect on Ud6-m-/p+ mice as compared with WT mice (**Figure 5**). During the exposure to LL, Ud6-m-/p+ mice displayed dramatically reduced activity levels and suppressed rhythms of wheel-running as compared with WT mice; most of Ud6-m-/p+ mice (5 out

of 8) were completely arrhythmic and displayed lower activity under LL (**Figure 5A**). The suppression of running-wheel activity largely recovered after mice were transferred from LL to DD (**Figure 5A**, left and middle panels). In addition, Ud6-m-/p+ mice had less general locomotion in both LL and after transfer from LL to DD as assessed by infrared sensors (**Figure 5B** left and middle panels). Moreover, the shortening of the circadian period of wheel-running behavior upon transfer from LL to DD was smaller in Ud6-m-/p+ than in WT mice (**Figure 5A**, right panel). While exposed to LL, the circadian periods of WT and Ud6-m-/p+ mice were comparable for both running-wheel activity (**Figure 5A** right) and for general activity (**Figure 5B** right), but after transfer to DD, the period of WT mice shortened  $\sim 1.5$  h ( $1.48 \pm 0.33$  h for running wheels,  $1.45 \pm 0.37$  h for general activity, right panels of **Figure 5**), whereas the LL to DD transfer evoked only  $\sim 1.0$ – $1.1$  h shortening in Ud6-m-/p+ mice ( $0.99 \pm 0.89$  h for running wheels,  $1.14 \pm 0.33$  h for general activity, right panels of **Figure 5**). The observation that LL-suppression of circadian amplitude is magnified while light-dependent period changes are diminished in Ud6-m-/p+ mice further supports our previous conclusion that normal levels of



UBE3A expression enhance circadian oscillator strength, and therefore that Angelman mice have weaker circadian pacemakers (Shi et al., 2015). In addition to altered circadian locomotor behavior in LL, the free running period of Angelman mice in DD trended toward longer periods when measured by rotating-saucer exercise wheels (Supplementary Figure 2). Together with our previously reported observations of Ud5-m/p+ mice (Shi et al., 2015), the data of Supplementary Figure 2 also imply a sex difference in the magnitude of period lengthening in Angelman mouse models.

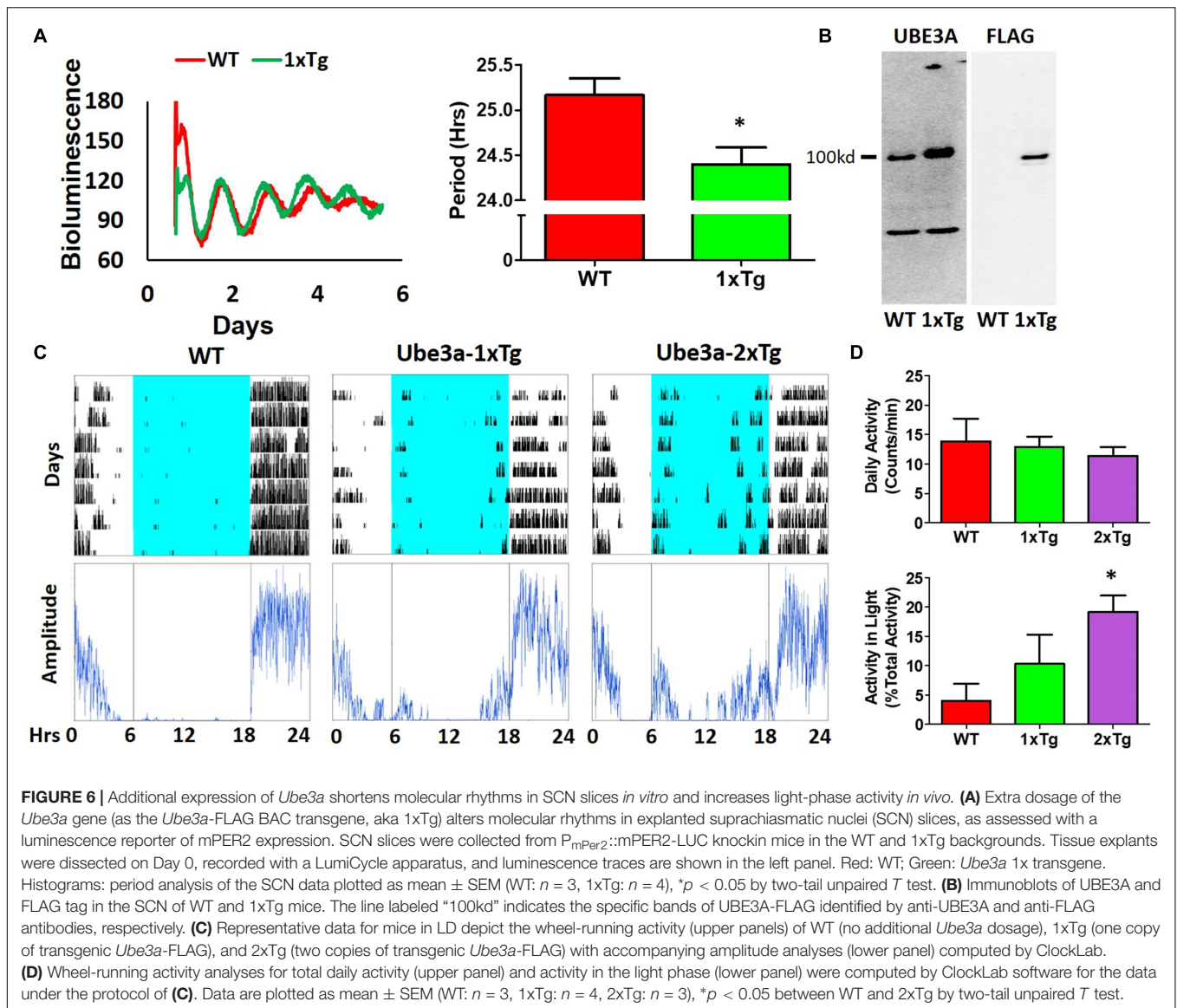
### Additional UBE3A Has Opposite Effects to UBE3A Deficiency on Clock Properties

Our observations of Ud6-m/p+ mice in this study and of Ud5-m/p+ mice in our previous study (Shi et al., 2015) indicate that the reduced expression of UBE3A in neurons leads to longer circadian periods and altered behavior in the light. What about enhanced expression of UBE3A? A simple prediction would be that additional expression of UBE3A should shorten the circadian period, and this is what we observed. Using ubiquitous overexpression of FLAG-*Ube3a* in a BAC transgenic mouse model for autism (Smith et al., 2011; Krishnan et al., 2017), we found that the circadian period of the SCN *in vitro* was shortened

by the enhanced expression of *Ube3a* compared with that in WT SCN from the same mixed background (Figure 6A). Ectopic UBE3A expression in the SCN from 1xTg mice was assessed by immunoblots, confirming that one additional copy of the *Ube3a* gene introduced by the FLAG-*Ube3a* transgene increased levels of UBE3A protein (Figure 6B). Moreover, while UBE3A deficiency in Angelman models suppresses the activity levels of mice in the light interval of LD (Figure 4; Shi et al., 2015), we found that *Ube3a* transgenic mice run more on wheels during the light/day phase of LD when the mice are usually inactive/asleep (Figures 6C,D), and this increased activity is *Ube3a* gene dosage-dependent; 2xTg mice displayed twice as much activity in the light interval as did 1xTg mice (Figure 6D).

### Reduced Stress Hormones and Anxiety in Ud6-m/p+ Mice

The reduced activity of Ud6-m/p+ mice in LL could be interpreted as an enhanced stress response to illumination. To rule out the possibility that this altered behavior was caused by stress or anxiety, we measured stress hormones and neurotransmitters in the serum and brain during the day phase of LD. Corticosterone and norepinephrine release are regulated by stress and the circadian clock (Le Minh et al., 2001;

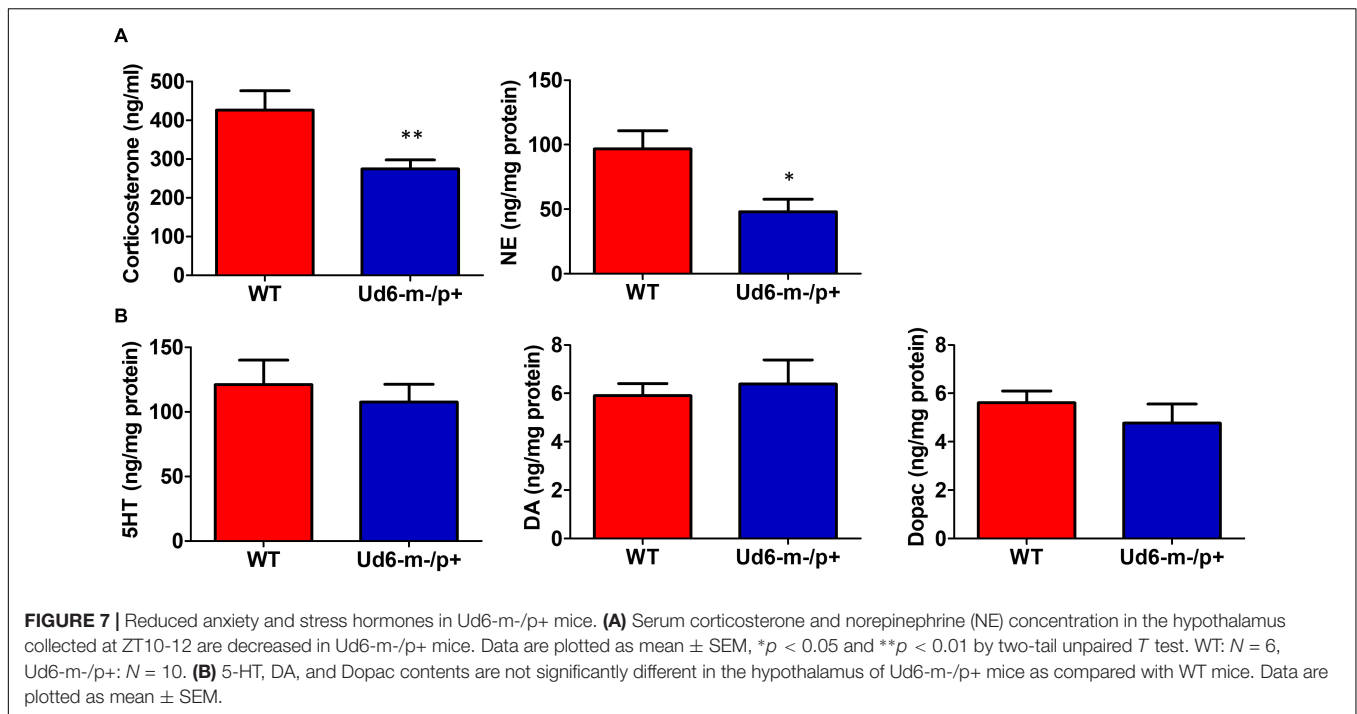


Ikegami et al., 2020). In Ud6-m-/p+ mice, we found that serum corticosterone levels are lower at ZT10-12 (Figure 7A), a peak phase for this hormone in the blood. Content of another stress-related hormone, norepinephrine, is similarly reduced in the hypothalamus of Ud6-m-/p+ mice at ZT10-12 (Figure 7A). We also found a reduced norepinephrine level in the cerebellum of Ud5-m-/p+ mice at the same early night phase (Supplementary Figure 3). In contrast, deficiency of *Ube3a* expression did not alter the levels of other key neurotransmitters (GABA, DA, DOPAC, and 5-HT) in the hypothalamus or the cerebellum (Figure 7B and Supplementary Figure 3). These decreased corticosterone and norepinephrine levels are consistent with the aforementioned results from the marble burying tests (Figure 4B) toward indicating a reduced behavioral anxiety in the Ud6-m-/p+ mice. Therefore, the anxiety/stress levels of Ud6-m-/p+ mice are less than—not greater—than those of WT mice, which is similar to the conclusions of studies with Angelman human

subjects (Robb et al., 1989), and consequently the reduced activity of Angelman model mice is probably not due to light-induced anxiety.

## Sleep and Siestas

Jones et al. (2016) reported that Ud5-m-/p+ mice have a blunted response to sleep pressure, both during their active period and in response to forced sleep deprivation. For example, Ud5-m-/p+ mice lack the small increase in sleep late in the active phase (“siesta”) that is typical of WT mice without access to running wheels. We similarly found that Ud6-m-/p+ mice skipped the siesta near the end of the dark interval when they did not have access to running wheels. Under LD 12:12 cycles, hourly assessments of wake, NREM sleep and REM sleep showed Ud6-m-/p+ mice had more wake, and less NREM sleep and REM sleep in this later part of the dark/night phase than did WT mice (Figure 8; ZT20,  $p = 0.017$  wake;  $p = 0.012$  NREM;  $p = 0.07$  REM).



Otherwise, Ud6-m-/p+ and WT mice had similar amounts of wake, NREM sleep, and REM sleep in both the dark and light periods. Ud6-m-/p+ mice also had fewer bouts of wake during the light period than WT mice (Table 1). Fast Fourier analysis of the EEG revealed Ud6-m-/p+ mice have lower delta power (0.25–0.75 Hz) across sleep and wake states (Supplementary Figure 4). Additionally, Ud6-m-/p+ mice have increased power in the 3–4.25 Hz range in wake (Supplementary Figure 4). Polyspike events with frequencies within the range of increased power in Ud6-m-/p+, and as described by Born et al. (2017), were observed throughout the EEG trace in Ud6-m-/p+ mice (Supplementary Figure 4).

On the other hand, the propensity to siesta reverses between WT and Ud6-m-/p+ mice when the mice have access to running wheels, which tend to promote arousal, likely due to increased overall activity (Edgar et al., 1991; España et al., 2007). When the mice are in LD 12:12 with access to a running wheel (rotating-saucer wheel, condition “LDRW”), hourly analyses suggested that Ud6-m-/p+ mice tend to have less wake and more NREM and REM sleep in the middle of the dark period (Figures 9A–C; WT vs. Ud6-m-/p+ were significantly different at ZT17,  $p = 0.045$ ). Ud6-m-/p+ and WT mice had similar numbers of bouts and durations of each stage across the 12 h dark and light intervals (Table 2). Interestingly, Ud6-m-/p+ mice had significantly lower core body temperature than WT mice during the dark phase (Figure 9D). Ud6-m-/p+ mice also exhibited less general activity (DSI) and running-wheel activity than WT mice during the dark phase of LD (Figures 9E,F).

Under constant dark conditions with access to a running wheel (condition “DDRW”), Ud6-m-/p+ mice had less wheel running than WT mice in the first part of the active phase, and their body temperature was correspondingly lower. Ud6-m-/p+

mice also had less wake and more NREM and REM sleep over this initial part of the active phase than WT mice (Supplementary Figure 5). Neither WT nor Ud6-m-/p+ mice had a siesta under the DDRW condition. Ud6-m-/p+ mice had less wake (vs. WT  $p = 0.03$ ) and more NREM sleep ( $p = 0.042$ ) at CT14. Ud6-m-/p+ mice also spent less time and had shorter REM sleep bout duration than WT mice during the subjective light (Supplementary Table 1). Overall, the lower amounts of wake in Ud6-m-/p+ mice during the early subjective dark period may be related to lower locomotor activity and body temperature.

## Sleep Deprivation

Jones et al. (2016) also reported that Ud5-m-/p+ mice have a reduced response to sleep deprivation. Typically, long periods of wake are followed by high EEG delta power in the subsequent NREM sleep. We found that after 6-h of sleep deprivation at the start of the light, Ud6-m-/p+ mice had lower delta power (0.25–4 Hz) in NREM sleep during the first hour of recovery sleep compared to WT mice (Supplementary Figure 6), though delta power then followed a normal pattern in the subsequent hours. Other measures of increased sleep pressure, including amount of time, number of bouts and duration of bouts of each state (wake, NREM sleep, and REM sleep) during recovery were similar between Ud6-m-/p+ and WT mice (Supplementary Table 2).

## DISCUSSION

The new Ud6-m-/p+ model has the potential to become a preferred rodent system for understanding AS. It combines the advantages of mouse genetics over the rat model of AS (Dodge et al., 2020) with the likelihood of enhanced stability and

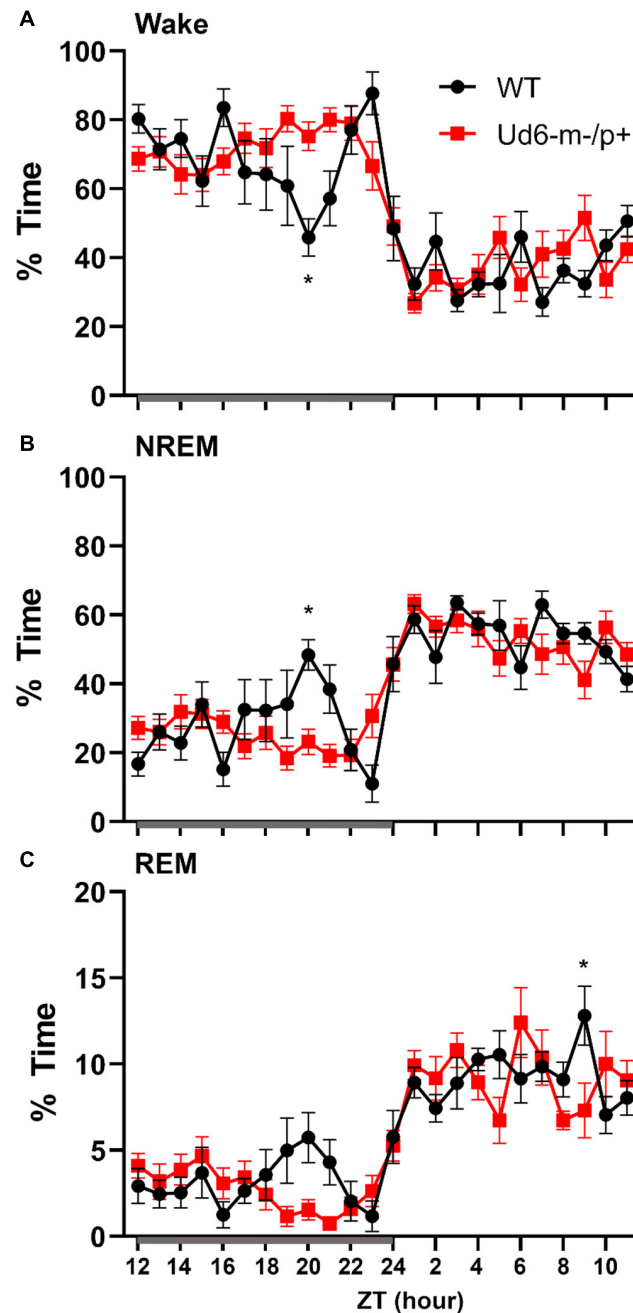


**FIGURE 8** | Sleep/wake behavior in WT and Ud6-m-/p+ mice in LD without access to running wheels. Amount of time in Wake (A), NREM sleep (B), and REM sleep (C) are similar in WT (black) and Ud6-m-/p+ mice (red) except that Ud6-m-/p+ mice have a blunted "siesta" episode late in the active (dark) interval. Darkness is indicated by the gray horizontal bar from ZT12-24. Data are plotted as mean  $\pm$  SEM. Asterisk (\*) indicates a significant difference between Ud6-m-/p+ vs. WT mice at the  $p < 0.05$  level.

consistency over the Ud5-m-/p+ model because of its 4X larger deletion (1247 nt). Moreover, Ud6-m-/p+ specifically targets the *Ube3a* gene so that its phenotypes can be attributed to that single gene, whereas a liability of the UG-m-/p+ model mouse is that two other genes are also affected, which complicates interpretations (Jiang et al., 2010). We confirmed that the Ud6-m-/p+ mouse exhibits standard phenotypes observed in the

other rodent models of AS (Jiang et al., 1998, 2010; Sonzogni et al., 2018; Dodge et al., 2020), such as worse coordination on rotarod and reduced marble burying (Figure 4).

In contrast to previous reports on the Ud5-m-/p+ mouse model (Ehlen et al., 2015; Jones et al., 2016), we clearly find much lower UBE3A protein expression in the SCN of Ud6-m-/p+ mice, thereby vindicating the expectation that *Ube3a*

**TABLE 1** | The number and duration of sleep and wake bouts in WT and Ud6-m-/p+ mice in LD without access to a running wheel (mean  $\pm$  SEM, \* $p < 0.05$ ).

		Amount (%)		# of bouts		Bout duration (sec)	
		12 h dark	12 h light	12 h dark	12 h light	12 h dark	12 h light
Wake	WT	69.2 $\pm$ 2	37.9 $\pm$ 1.3	136.3 $\pm$ 26.5	176.1 $\pm$ 14.1	264.6 $\pm$ 38.6	97.1 $\pm$ 8.1
	Ud6-m-/p+	72 $\pm$ 2	38.8 $\pm$ 2	112.5 $\pm$ 5.8	<b>141.3 <math>\pm</math> 5.5*</b>	282.9 $\pm$ 18.6	124.0 $\pm$ 9.1
NREM	WT	27.7 $\pm$ 1.7	53.2 $\pm$ 1.2	132.9 $\pm$ 26.9	181.6 $\pm$ 16.7	107.1 $\pm$ 13.0	131.1 $\pm$ 7.8
	Ud6-m-/p+	25.3 $\pm$ 1.9	52.3 $\pm$ 2	110.8 $\pm$ 5.6	154.3 $\pm$ 6.3	106.2 $\pm$ 9.2	142.4 $\pm$ 6.7
REM	WT	3.1 $\pm$ 0.3	9 $\pm$ 0.2	29.9 $\pm$ 3.5	67.3 $\pm$ 5.5	48.8 $\pm$ 5.5	59.8 $\pm$ 4.1
	Ud6-m-/p+	2.7 $\pm$ 0.3	8.9 $\pm$ 0.7	27.3 $\pm$ 3.7	67.5 $\pm$ 4.1	46.0 $\pm$ 3.4	57.0 $\pm$ 2.5

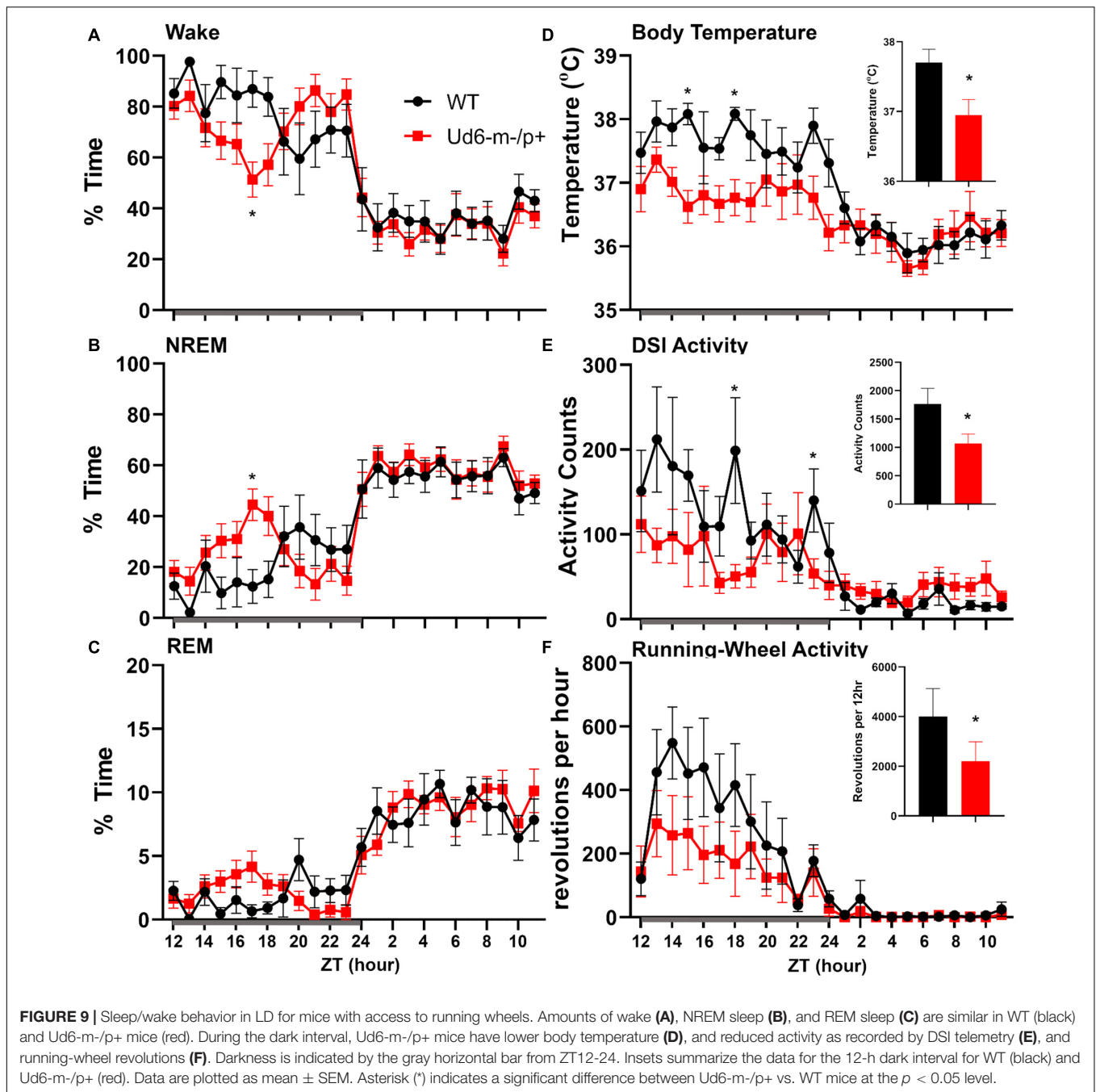
Sleep data under LD conditions without access to running wheels. \* and emboldened text indicate difference between Ud6-m-/p+ vs. WT at level of  $p < 0.05$  unpaired T-test.

is imprinted in neurons, and that SCN neurons are not exceptional in that regard. These differing conclusions may be due to the aforementioned tendency of the Ud5-m-/p+ model toward strain dependency and loss of phenotype over time (Huang et al., 2013; Born et al., 2017). Another source of the discrepancy in apparent expression of UBE3A in the SCN may be due to different methods. The study of Jones et al. (2016) used the NeuN marker to identify neurons, but the accuracy of this particular marker for neurons in the SCN has been questioned by Morin et al. (2011). Apparently NeuN-positive neurons represent only a subpopulation of neurons with a specific spatial distribution in the mouse SCN (Morin et al., 2011), and therefore the use of NeuN may overlook a large population of SCN neurons. In contrast, our IHC utilized an antibody to the neuron-specific RNA-binding protein, ELAVL4/HuD that has been used successfully as a global marker of neuronal cells in brain tissues (Jung and Lee, 2021). Finally, our assessment of UBE3A expression in the SCN was based on the more stringent criterion of “number of UBE3A-positive cells,” and we found that 25% of SCN cells retain a low level of UBE3A expression (Figure 3C). Why? Recent research may provide an explanation for this heterogeneity within the SCN as approximately 20–30% of SCN cells are neither neurons nor astrocytes (Wen et al., 2020; Morris et al., 2021; Xu et al., 2021). Using the ELAVL4 antibody to define which cells are neuronal vs. non-neuronal (Jung and Lee, 2021), we found that SCN neurons of the Ud6-m-/p+ mouse have significantly reduced expression of UBE3A (Supplementary Figure 1). Moreover, it seems likely that some of the UBE3A-positive cells are not neurons or astrocytes, but represent oligodendrocytes, endothelial or ependymal cell types that do not paternally imprint *Ube3a* (Yamasaki et al., 2003; Jiang et al., 2010; Grier et al., 2015). Therefore, our conclusion is that UBE3A expression is dramatically suppressed in SCN neurons of Ud6-m-/p+ mice, and therefore the paternal *Ube3a* gene is imprinted in SCN neurons as expected from studies of neurons in other brain regions (Albrecht et al., 1997; Jiang et al., 1998; Weeber et al., 2003).

We previously reported that circadian robustness was impaired in the Ud5-m-/p+ and UG-m-/p+ mouse models of AS (Shi et al., 2015). Here, we show that the Ud6-m-/p+ model shares these same phenotypes, especially the suppressed locomotor activity in LL (Figure 5). We also observed depressed

locomotor activity rhythms (both running wheel and total DSI activity) in LD and DD (Figure 9 and Supplementary Figure 4). Consequently, we observe significant circadian phenotypes in all three mouse models of Angelman syndrome, and our results concur with an earlier circadian study of the roles of *Ube3a* in tissue cultures (Gossan et al., 2014). Inexplicably, Ehlen et al. (2015) could not repeat our prior observation of lengthened circadian periods in Ud5-m-/p+ mice (although their data showed a trend toward lengthening, the difference was not statistically significant). We attribute these differences to unidentified differences in the conditions under which the rhythms were monitored in the various labs, or to the lability of the Ud5-m-/p+ model, including a potential loss of phenotype over time that might have affected the mice in other labs (Huang et al., 2013; Born et al., 2017; Dodge et al., 2020). Our observations here with the Ud6-m-/p+ mouse model reaffirms that *Ube3a* deficiency has circadian ramifications. The present study also demonstrates reciprocal effects of *Ube3a* gene dosage on the circadian system. When UBE3A levels are reduced in neurons due to paternal imprinting, light suppresses wheel-running activity and the circadian period lengthens (Figure 5; Shi et al., 2015). Conversely, light enhances the activity when mice are in the light, and the circadian period of the cultured SCN clock *in vitro* is shorter when *Ube3a* is over-expressed in an autism mouse model (Figure 6). Therefore, the circadian clock is inversely sensitive to loss and gain of *Ube3a* expression, supporting an important homeostatic action for UBE3A in the circadian clockwork.

Children with Angelman syndrome often have nighttime awakenings and difficulty initiating sleep (Trickett et al., 2017). In mouse models of Angelman syndrome, two previous studies reported altered sleep patterns in an Angelman syndrome mouse line (Ehlen et al., 2015; Copping and Silverman, 2021). Ehlen et al. (2015) reported a lack of the “siesta-like” reduction of wake in the late night/active bout of Ud5-m-/p+ mice compared to WT mice. Similarly, under LD conditions in our experiments, Ud6 m-/p+ mice did not show this siesta which was clear in WT mice around ZT20 (Figure 8). Interestingly, when a running wheel is present, the Ud6-m-/p+ mice are active later in the dark/night interval (Figure 9A), which is a phased activity pattern reminiscent to that we reported for Ud5-m-/p+ mice (Shi et al., 2015) and which we attributed to the entrainment of a longer free-running period to LD. Still, even with access to a running wheel, Ud6-m-/p+ mice



had lower core body temperature, most likely due to less wheel running than their WT littermates (Figures 9D–F).

Increased EEG delta power during wake and sleep has been reported in children with AS and a mouse model of AS (Sidorov et al., 2017; den Bakker et al., 2018), whereas lower delta power late in the dark period was reported for the Ud5-m-/p+ mouse model by Ehlen et al. (2015). The increased high delta/low theta power observed in the Ud6-m-/p+ mice is similar to previous reports of altered power distribution in the EEG of *Ube3a* deficient mice. Born et al. (2017) reported increased theta power in *Ube3a* maternal deficient mice and attributed this increase to

polyspike events in cortical and hippocampal EEG traces. We also observed polyspike events in our cortical EEG recordings mainly in wake and REM sleep, with fewer in NREM sleep. These events may indicate a predisposition for seizure activity, but we did not observe overt seizures in these mice (Born et al., 2017). Unfortunately, Born et al. (2017) did not separate the power spectrum analysis by state of arousal and so comparisons between studies are difficult. The low delta power observed in the Ud6-m-/p+ mice differ from other groups, however, the differences in scoring stages of wake and sleep may account for some of the discrepancy, in addition to different genetics of the

**TABLE 2** | The number and duration of sleep and wake bouts in WT and Ud6-m-/p+ mice in LD with access to a running wheel (mean ± SEM).

		Amount (%)		# of bouts		Bout duration (sec)	
		12 h dark	12 h light	12 h dark	12 h light	12 h dark	12 h light
Wake	WT	78.3 ± 4.1	36.4 ± 2.4	73.5 ± 14.5	159.5 ± 33.5	479.9 ± 134.7	95.9 ± 19.9
	Ud6-m-/p+	73 ± 1.9	33.3 ± 2.3	67 ± 17.3	137.8 ± 25.0	711.3 ± 224.3	111.8 ± 16.7
NREM	WT	19.9 ± 3.7	55.3 ± 2.5	64 ± 18	163.5 ± 28.5	144.2 ± 0.5	162.2 ± 33.6
	Ud6-m-/p+	24.9 ± 1.8	58 ± 2.2	59.4 ± 17.5	151.8 ± 19.6	146.5 ± 17.1	187.9 ± 47.3
REM	WT	3.3 ± 1	9.4 ± 1.2	12 ± 1	47.5 ± 20.5	55.9 ± 30.5	64.1 ± 2.3
	Ud6-m-/p+	2.1 ± 0.2	8.6 ± 0.3	10.2 ± 4.2	65.2 ± 7.6	42.8 ± 9.5	62.4 ± 10.4

Sleep data under LDRW conditions (= LD with access to a running wheel).

AS models. Moreover, Jones et al. (2016) reported that Ud5-m-/p+ mice have a reduced capacity to accumulate sleep pressure in response to sleep deprivation; typically, increasing duration of wake increases EEG delta power in the subsequent NREM sleep. We found that Ud6-m-/p+ mice had lower delta power during their initial NREM sleep after 6-h of sleep deprivation, suggesting some blunting of the response to sleep pressure.

Ud6-m-/p+ mice also differed in their pattern of REM sleep. We found that Ud6-m-/p+ had ~30% less REM sleep amount during the subjective day of DD (with access to a running-wheel), most likely due to shorter bouts of REM sleep. Similarly, a prior study reported that Ud5-m-/p+ mice had about 20% less REM sleep across the 24-h day (Ehlen et al., 2015). Though their scoring methods differ, Copping and Silverman (2021) also report less REM sleep in *Ube3a* null mice. Future research in people with AS might target whether their fragmented sleep disrupts REM sleep.

Pharmacological and genetic studies in mammals suggest that norepinephrine plays a critical role in promoting arousal, especially during conditions that require high attention or activation of the sympathetic nervous system (España and Scammell, 2011). Moreover, corticosteroid therapy benefits children with Angelman syndrome (Forrest et al., 2009). We detected reduced norepinephrine in the hypothalamus of Ud6-m-/p+ mice during the late day (ZT10-12 in **Figure 7**), which correlates with a decreased wake during the subsequent night (ZT17 in **Figure 9**). Reduced levels of norepinephrine during the early subjective night (CT14 of DD) in Ud5-m-/p+ cerebellum is also in line with decreased wakefulness during early night in Ud6-m-/p+ animals (**Supplementary Figures 3, 4**). Low norepinephrine is also associated with drowsy and inattentive behaviors in mammals (España and Scammell, 2011), which correlates with symptoms of Angelman patients (Pelc et al., 2008). Stress hormones, including corticosterone and norepinephrine, are released during and immediately after stressful stimuli tested in emotionally arousing learning tasks (Aston-Jones and Cohen, 2005). Moreover, removal of these hormones by adrenalectomy impairs memory consolidation for emotionally arousing experiences (Foote et al., 1980; Roozendaal, 2002). Observations from human AS patients correlate well with our measurements indicating depleted levels of corticosterone and norepinephrine in *Ube3a* deficient mice (Kim et al., 2018), and may represent a partial explanation for compromised cognition and impaired learning and memory in AS. Taken together, the

hypothalamic-pituitary-adrenal (HPA) axis and may represent new therapeutic targets to ameliorate AS phenotypes. Moreover, cortisol and norepinephrine may serve as easily measurable biomarkers for assessing the efficacy of potential therapeutic treatments of Angelman syndrome in clinical trials.

Although animal models can never fully recapitulate the complexity of clinically important human syndromes, they can provide key resources for analyses. In this case, mouse models of Angelman syndrome help to identify the mechanistic consequences of alterations of *Ube3a* expression levels that result in Angelman syndrome when deficient versus autism when over-abundant. The impact of *Ube3a* under- and over-expression is considerable upon human neurodevelopment and sleep, and the new Ud6-m-/p+ mouse provides an experimentally tractable model to analyze sleep and the underlying regulation by the circadian system.

## MATERIALS AND METHODS

### Mouse Strains

C57BL/6J mice harboring a knockout of exon 6 of the *Ube3a* gene were generated with CRISPR/Cas9 (**Figure 1A**), and this strain is herein called “Ud6-m-/p+.” We confirmed that the Ud6-m-/p+ strain in our mouse colonies was genetically 98.97% (289/292 SNPs) C57BL/6J (JAX# 000664), as assessed by genotyping performed by the Jackson Laboratory (Bar Harbor, ME, United States). Female mice harboring one *Ube3a* knockout allele were crossed with wild-type background (WT C57BL/6J) male mice to obtain the maternal deletion mice (Ud6-m-/p+) that are the model for Angelman syndrome. “Ud5-m-/p+” represents the original Angelman model mouse strain harboring an exon 5 deletion in *Ube3a* (Jiang et al., 1998).

*Ube3a* conventional BAC overexpressing mouse models (*Ube3a*-Tg 1x) on the FVB background (Smith et al., 2011; Krishnan et al., 2017) were crossed with C57Bl6 WT or Per2::Luc mice to generate an F1 generation with a mixed genetic background to obtain the WT, *Ube3a*-Tg 1x, and *Ube3a*-Tg 2x strains shown in **Figure 6**. As reported by other research groups for “Angelman phenotypes” (Huang et al., 2013; Born et al., 2017), we also found that mouse genetic backgrounds have significant effects on circadian properties, e.g., the period of the SCN rhythm *in vitro* displayed a lengthened circadian period

on the FVB/C57BL/6 mixed background (**Figure 6A**) compared with that on the C57BL/6 background (Shi et al., 2015).

Age and sex balanced experimental and littermate control mice were used in all animal assays (age range of 3–6 months). At Vanderbilt University, mice were housed in temperature-controlled environments on LD 12:12 (12:12-h light-dark cycle with lights-on at 06:00, cool-white fluorescence light ~ 300 lux) and fed chow (5001, Lab diet, 5% fat) for breeding and experiments. All animal experiments were approved by the Vanderbilt University and Beth Israel Deaconess Medical Center Institutional Animal Care and Use Committees and were conducted according to those committees' guidelines.

## Immunoblotting and Quantitative Reverse Transcription PCR

Animals were sacrificed by cervical dislocation at ZT4 in LD 12:12. The cerebellum samples were collected and stored at  $-80^{\circ}\text{C}$  until protein and RNA were extracted. Tissues were sonicated in RIPA buffer containing a cocktail of protease inhibitors (Sigma, St. Louis, MO, United States) and clarified by centrifugation (RIPA buffer = 50 mM Tris pH 8.0, 150 mM NaCl, 0.1% SDS, 1.0% NP-400, 5% Sodium Deoxycholate). Protein from the supernatant was quantified by the Bradford assay (Bio-Rad, Hercules, CA, United States). Proteins were separated by SDS-PAGE and then transferred to PVDF membranes for immunoblotting. Monoclonal IgG directed against UBE3A protein (E8655, Sigma) and anti- $\beta$ -ACTIN monoclonal antibody (A5316, Sigma) were used to probe UBE3A and  $\beta$ -ACTIN, respectively. To test the UBE3A and FLAG tag transgenic expression in the SCN, protein extracts from SCN cultures were examined by SDS-PAGE immunoblotted with anti-UBE3A monoclonal antibody (E8655, Sigma), or anti-FLAG monoclonal antibody (F1804, Sigma). Densitometric analyses were performed using Image J software (NIH).

Total cerebellum RNA collected at ZT4 were extracted and transcribed by Superscript III reverse transcriptase (Invitrogen, Carlsbad, CA, United States) following the manufacturer's instructions. Diluted cDNA was amplified by PCR using the SYBR Green Master Mix (Sigma), and raw threshold-cycle time (Ct) values were calculated with iQ5 software (Bio-Rad). Mean values were calculated from samples and normalized to those obtained for *Hprt* transcripts as reported previously (Shi et al., 2015).

## Marble Burying and Rotarod Assay

In order to assess anxiety and compulsiveness, Ud6-m-/p+ mice were placed in individual cages containing ~5 cm of diamond soft bedding (Teklad 7089C) at ZT3-5 for 15 min to acclimate to the test conditions, which were in the light (mice in subjective daytime). After 15 min, each mouse was briefly removed from its cage, and twenty-five marbles (~1.5 cm) were placed in the cage in 5 rows. The mice were returned to the cage and allowed 30 min to investigate the marbles. The number of marbles buried at least two-thirds of the way in the bedding was recorded. To test the anxiety during the night phase, mice from their home cage at ZT15-17 were transferred to a testing cage in the dark under

infrared illumination. The mice were tested in the dark (mice in subjective nighttime) in the test cage with marbles in diamond soft bedding. After 30 min, mice were returned to their home cages in the dark under infrared illumination, and the number of marbles buried in the bedding is recorded.

The ability to maintain balance on a rotating cylinder is measured with a standard rotarod apparatus (Ugo Basile, Gemonio, Italy), consisting of a cylinder (approx. 3 cm in diameter) that rotates at speeds ranging from 4 to 40 rpm in 5 min. Mice are placed on the rotarod and confined to a section of the cylinder approximately 6.0 cm wide by Plexiglas dividers. The latency at which mice fall off the rotating cylinder is automatically measured. Rotarod performance was assessed three times daily during ZT8-11 for two contiguous days.

## Per2::Luc Organotypic Slice Bioluminescence Assays

Mice harboring the  $P_{mPer2::mPER2-LUC}$  knock-in allele (Yoo et al., 2004) that have been backcrossed with the C57BL/6J strain for more than 12 generations were crossed with the *Ube3a* BAC transgenic mice (FVB background) to obtain *Ube3a*-Tg 1x with the luminescence reporter of mPER2 expression. The data in **Figure 6** were measured from these mixed background mice in the F1 generation so that they were 50% FVB and 50% C57BL/6J. One to 2 h before lights-off of LD 12:12, the mice were sacrificed by cervical dislocation, and cultures of SCN and peripheral tissues were prepared as previously described (Shi et al., 2015). The tissues were cultured in recording medium containing 10% fetal bovine serum (Gibco, Grand Island, NY, United States) and 100 nM of luciferin (Promega, Madison, WI, United States) at  $36.5^{\circ}\text{C}$ . The *in vitro* rhythms were analyzed using LumiCycle analysis software (Actimetrics, Evanston, IL, United States).

## Determination of Biogenic Amine and Corticosterone Concentration

The Ud6-m-/p+ and WT hypothalamus and serum samples were collected from mice sacrificed at ZT10-12 in LD 12:12. The Ud5-m-/p+ and WT cerebellum samples were collected from mice in DD for 26 and 38 h. Biogenic monoamines in hypothalamus and cerebellum were analyzed using LC/MS by the Neurochemistry Core Laboratory of Vanderbilt University Medical Center, and the samples were normalized to total protein concentration. The corticosterone concentration in serum was analyzed using double antibody RIA by the Hormone Assay and Analytics Core Laboratory of Vanderbilt University Medical Center.

## Immunohistochemistry

The animals were deeply anesthetized by Avertin (1.25%, Sigma) and perfused in PFA (4% in PBS, Sigma). Brains were removed and postfixed in 4% PFA for 12 h at  $4^{\circ}\text{C}$ , and cryoprotected in 20% sucrose-PBS overnight at  $4^{\circ}\text{C}$ . Coronal 30- $\mu\text{m}$ -thick sections were cut on a freezing microtome (CM1850, Leica, Germany) and free-floating sections were processed for standard avidin-biotin IHC and immunofluorescence methods as previously described (Sumová et al., 2002; Liska et al., 2021). The sections were incubated in 0.5% peroxide solution in PBS

(0.01 M sodium phosphate- 0.15 M NaCl, pH 7.2) for 10 min for peroxidase blocking. For the immunofluorescence, this step was skipped. Then, the sections were incubated in 2% normal goat serum (Vector Laboratories, United States) + 1% bovine serum albumin (Sigma, United States) + 0.3% Triton X-100 (Sigma, United States) for 60 min.

The primary polyclonal antibodies applied overnight at 4°C were as follows: mouse anti-UBE3A 1: 600 (SAB1404508, Sigma, United States); rabbit anti-ELAVL4/HuD 1: 600 (ab96474, Abcam, Great Britain, United Kingdom) as a neuronal marker (Okano and Darnell, 1997; Loffreda et al., 2020); chicken anti-GFAP 1: 1000 (ab4674, Abcam, Great Britain, United Kingdom) as a brain astrocyte marker (Brenner et al., 1994). For the immunofluorescence IHC, the secondary antibodies (1: 600; 1 h) were goat anti-mouse fluorescent (F2761, Thermo Fischer Scientific, United States), goat anti-rabbit fluorescent (A11037, Thermo Fischer Scientific, United States), and goat anti-chicken fluorescent (ab97145, Abcam, Great Britain, United Kingdom). The immunofluorescence was visualized using confocal microscopy (Multiphoton Microscope Leica TCS SP8 MP, Leica, Germany).

For the avidin-biotin IHC, we applied standard methods with diaminobenzidine tetrahydrochloride (Sigma, United States) as the chromogen (Vector Laboratories, Peterborough, United Kingdom). For quantification, cell nuclei labeled irrespective of the intensity of their staining were counted in the whole SCN (3–9 sections per brain) by a “procedure-blind” person using an image analysis system (ImageJ/FUJI). In the hippocampal regions, where cell bodies are dense and difficult to reliably resolve, optical staining density was measured (3–5 sections per brain) rather than counting individual cells for positive staining. After conversion of the images into gray scale, the optical density measurement was performed selectively in CA1, CA3, and DG regions and in the closely adjacent areas without cell bodies. The optical density (gray color intensity) was calculated as follows:  $OD = \log(\text{background intensity}/\text{cells intensity})$ . For the density measurements, the sections from WT and Ud6-m-/p+ mice were assayed simultaneously in one IHC assay.

## Sleep Electroencephalogram Procedures

For sleep EEG measurements at the Beth Israel Deaconess Medical Center, male and female mice were housed on LD 12:12 (lights on at 07:00) with constant temperature ( $22 \pm 1.4^\circ\text{C}$ ) and humidity ( $26 \pm 2.1$  mmHg). Regular chow (LabDiet #5058) and water were available *ad libitum*. Mice were  $16.4 \pm 0.9$  weeks old and weighed  $25.4 \pm 0.5$  g at the time of surgery. We anesthetized mice with ketamine/xylazine (100/10 mg/kg, i.p.) and placed them in a stereotaxic alignment system (model 1900; Kopf Instruments). Electroencephalogram (EEG) and electromyogram (EMG) electrodes were soldered to a  $2 \times 2$  pin microstrip connector and implanted and affixed to the skull with dental cement for polysomnogram recordings. For the EEG electrodes, two stainless steel screws were implanted into the skull 1.5 mm lateral and 0.5 mm rostral to bregma and 1.0 mm rostral to lambda. The EMG electrodes were made from multistranded stainless steel wire (Cooner Wire) and placed into the neck

extensor muscles. We treated each mouse with meloxicam (4 mg/kg slow release, s.c.) at the time of surgery.

## Sleep Recordings

One week after implantation of EEG and EMG electrodes, we transferred mice to recording cages in a sound-attenuated box. We attached the recording cable to a low-torque electrical swivel that was fixed to the cage top to allow free movement. We allowed the mice 7 days to habituate to the recording cable and chamber. EEG/EMG signals were amplified, filtered (high-pass, 0.3 Hz; low-pass, 1 kHz), digitized at a sampling rate of 256 Hz, and recorded with SleepSign software (Kissei Comtec). We used SleepSign (filter settings: EEG, 0.25–64 Hz; EMG, 10–60 Hz) for preliminary, semiautomatic scoring of wake, REM, and non-REM (NREM) sleep in 10 s epochs and then examined all epochs and made corrections when necessary.

We recorded sleep/wake behavior under 4 conditions for WT ( $n = 8$ ) and Ud6-m-/p+ ( $n = 12$ ). Twenty-four-hour sleep recordings were first acquired under LD 12:12 conditions, after which time the response of the mice to sleep deprivation was assessed. At the start of the light phase, mice were kept awake for 6 h by introducing novel objects into the cage or by lightly tapping on the side of the cage, and subsequently behavior across the 6-h recovery period after the sleep deprivation was recorded. Then, mice were acclimated to running wheels for 10 days and 24-h sleep recordings were acquired in the “LD with running wheel” (LDRW) condition. Finally, mice were held in constant dark (DD) for at least 14 days prior to performing 24-h sleep recordings under “DD with running wheel” (DDRW) condition. RW, LMA and Tb data were analyzed using ClockLab (Coulbourn Instruments, Natick, MA, United States) to analyze period (Chi-squared periodogram) and cosinor amplitude for the last 7 days in LD and the last 7 days in DDRW. Two-way repeated measures ANOVA was used to compare between genotypes with Bonferroni tests for multiple comparisons serving as *post hoc* analyses. For DDRW sleep data plots, running wheel onset were manually determined to align the start of subjective dark.

## Circadian Locomotor Behavior Measurement

For the circadian behavioral experiments performed at Vanderbilt University, age- and gender-matched littermates were singly housed in cages equipped with running-wheel or infrared sensors for locomotor activity measurements with unlimited access to regular chow (5001, Lab diet) and water. For the running wheel experiments shown in **Figure 8**, a rotating-saucer running-wheel was used to measure the locomotor activity at Beth Israel Deaconess Medical Center. ClockLab software (Actimetrics, Evanston, IL, United States) was used to collect data and perform period and activity analyses. Circadian periods in DD and LL were calculated using Chi-Square periodogram analyses.

## Statistical Analyses

Data are presented as means  $\pm$  SEM. Statistical analyses were performed by two-tail unpaired *t*-test, one-way, and two-way

ANOVA as indicated (GraphPad, PRISM9). For sleep EEG, we analyzed light and dark period data between mutants and WT littermates using unpaired *T*-tests. Hourly data was assessed with two-way ANOVA (time  $\times$  genotype) and *post hoc* Bonferroni tests were run to adjust for multiple comparisons (GraphPad, PRISM9). Recovery sleep NREM spectra was analyzed with area under the curve including frequencies of 0.25–4 Hz.

## DATA AVAILABILITY STATEMENT

The original contributions presented in the study are included in the article/**Supplementary Material**, further inquiries can be directed to the corresponding author.

## ETHICS STATEMENT

The animal study was reviewed and approved by the Vanderbilt University and Beth Israel Deaconess Medical Center Institutional Animal Care and Use Committees and was conducted according to those committees' guidelines.

## AUTHOR CONTRIBUTIONS

S-QS and CM designed and performed the experiments, analyzed the data, and wrote and edited the manuscript. PH performed the experiments and analyzed the data. WZ performed the experiments. MA provided materials. XZ performed the experiments and provided materials. AB provided materials and information. AS and TS designed and supervised the experiments in the study, and edited the manuscript. CJ was responsible for

overall supervision of the study, designed the experiments, and wrote and edited the manuscript. All authors contributed to the article and approved the submitted version.

## FUNDING

This work was supported by funding from the United States National Institutes of Health (R01 NS104497 to CJ and TS, R01 NS106032 to TS, and R01MH112714 and R01MH114858 to MA). AS thanks MEYS (LM2015062 Czech-BioImaging) for support. The Vanderbilt Murine Neurobehavior Core Lab (U54HD083211, NICHD) assisted in the performance of the Rotarod and Marble Burying testing, Vanderbilt Neurochemistry Core Lab assayed biogenic amines, and Vanderbilt Hormone Assay and Analytics Core Laboratory (DK059637 and DK020593, NIDDK) determined corticosterone levels.

## ACKNOWLEDGMENTS

We thank N. Machado and W. Todd for technical assistance with the sleep studies, and Dan Cai for assistance with breeding Angelman model mice. We are grateful to Terri Jo Bichell for inspiring us to study circadian rhythms and sleep in Angelman models.

## SUPPLEMENTARY MATERIAL

The Supplementary Material for this article can be found online at: <https://www.frontiersin.org/articles/10.3389/fnbeh.2022.837523/full#supplementary-material>

## REFERENCES

- Albrecht, U., Sutcliffe, J. S., Cattanach, B. M., Beechey, C. V., Armstrong, D., Eichele, G., et al. (1997). Imprinted expression of the murine Angelman syndrome gene, *Ube3a*, in hippocampal and Purkinje neurons. *Nat. Genet.* 17, 75–78. doi: 10.1038/ng0997-75
- Angoa-Pérez, M., Kane, M. J., Briggs, D. I., Francescutti, D. M., and Kuhn, D. M. (2013). Marble burying and nestlet shredding as tests of repetitive, compulsive-like behaviors in mice. *J. Visual. Exp.* 82:e50978. doi: 10.3791/50978
- Aston-Jones, G., and Cohen, J. D. (2005). An integrative theory of locus coeruleus-norepinephrine function: adaptive gain and optimal performance. *Annu. Rev. Neurosci.* 28, 403–450.
- Born, H. A., Dao, A. T., Levine, A. T., Lee, W. L., Mehta, N. M., Mehra, S., et al. (2017). Strain-dependence of the Angelman syndrome phenotypes in *Ube3a* maternal deficiency mice. *Sci. Rep.* 7, 1–15. doi: 10.1038/s41598-017-08825-x
- Brenner, M., Kisseberth, W. C., Su, Y., Besnard, F., and Messing, A. (1994). GFAP promoter directs astrocyte-specific expression in transgenic mice. *J. Neurosci.* 14, 1030–1037. doi: 10.1523/JNEUROSCI.14-03-01030.1994
- Colas, D., Wagstaff, J., Fort, P., Salvat, D., and Sarda, N. (2005). Sleep disturbances in *Ube3a* maternal-deficient mice modeling Angelman syndrome. *Neurobiol. Dis.* 20, 471–478. doi: 10.1016/j.nbd.2005.04.003
- Copping, N. A., and Silverman, J. L. (2021). Abnormal electrophysiological phenotypes and sleep deficits in a mouse model of Angelman Syndrome. *Mol. Autism* 12, 1–14. doi: 10.1186/s13229-021-00416-y
- den Bakker, H., Sidorov, M. S., Fan, Z., Lee, D. J., Bird, L. M., Chu, C. J., et al. (2018). Abnormal coherence and sleep composition in children with Angelman syndrome: a retrospective EEG study. *Mol. Autism* 9, 1–12. doi: 10.1186/s13229-018-0214-8
- Dindot, S. V., Antalffy, B. A., Bhattacharjee, M. B., and Beaudet, A. L. (2008). The Angelman syndrome ubiquitin ligase localizes to the synapse and nucleus, and maternal deficiency results in abnormal dendritic spine morphology. *Hum. Mol. Genet.* 17, 111–118. doi: 10.1093/hmg/ddm288
- Dodge, A., Peters, M. M., Greene, H. E., Dietrick, C., Botelho, R., Chung, D., et al. (2020). Generation of a novel rat model of Angelman Syndrome with a complete *Ube3a* gene deletion. *Autism Res.* 13, 397–409. doi: 10.1002/aur.2267
- Edgar, D. M., Kilduff, T. S., Martin, C. E., and Dement, W. C. (1991). Influence of running wheel activity on free-running sleep/wake and drinking circadian rhythms in mice. *Physiol. Behav.* 50, 373–378.
- Ehlen, J. C., Jones, K. A., Pinckney, L., Gray, C. L., Burette, S., Weinberg, R. J., et al. (2015). Maternal *Ube3a* loss disrupts sleep homeostasis but leaves circadian rhythmicity largely intact. *J. Neurosci.* 35, 13587–13598. doi: 10.1523/JNEUROSCI.2194-15.2015
- España, R. A., McCormack, S. L., Mochizuki, T., and Scammell, T. E. (2007). Running promotes wakefulness and increases cataplexy in orexin knockout mice. *Sleep* 30, 1417–1425. doi: 10.1093/sleep/30.11.1417
- España, R. A., and Scammell, T. E. (2011). Sleep neurobiology from a clinical perspective. *Sleep* 34, 845–858. doi: 10.5665/SLEEP.1112
- Foote, S. L., Aston-Jones, G., and Bloom, F. E. (1980). Impulse activity of locus coeruleus neurons in awake rats and monkeys is a function of sensory stimulation and arousal. *Proc. Nat. Acad. Sci.* 77, 3033–3037. doi: 10.1073/pnas.77.5.3033

- Forrest, K. M., Young, H., Dale, R. C., and Gill, D. S. (2009). Benefit of corticosteroid therapy in Angelman syndrome. *J. Child Neurol.* 24, 952–958. doi: 10.1177/0883073808331344
- Goldman, S. E., Bichell, T. J., Surdyka, K., and Malow, B. A. (2012). Sleep in children and adolescents with Angelman syndrome: association with parent sleep and stress. *J. Intell. Disabil. Res.* 56, 600–608. doi: 10.1111/j.1365-2788.2011.01499.x
- Gossan, N. C., Zhang, F., Guo, B., Jin, D., Yoshitane, H., Yao, A., et al. (2014). The E3 ubiquitin ligase UBE3A is an integral component of the molecular circadian clock through regulating the BMAL1 transcription factor. *Nucleic Acids Res.* 42, 5765–5775. doi: 10.1093/nar/gku225
- Grier, M. D., Carson, R. P., and Lagrange, A. H. (2015). Toward a broader view of Ube3a in a mouse model of Angelman syndrome: expression in brain, spinal cord, sciatic nerve and glial cells. *PLoS One* 10:e0124649. doi: 10.1371/journal.pone.0124649
- Gustin, R. M., Bichell, T. J., Bubser, M., Daily, J., Filonova, I., Mrelashvili, D., et al. (2010). Tissue-specific variation of Ube3a protein expression in rodents and in a mouse model of Angelman syndrome. *Neurobiol. Dis.* 39, 283–291. doi: 10.1016/j.nbd.2010.04.012
- Huang, H. S., Burns, A. J., Nonneman, R. J., Baker, L. K., Riddick, N. V., Nikolova, V. D., et al. (2013). Behavioral deficits in an Angelman syndrome model: effects of genetic background and age. *Behav. Brain Res.* 243, 79–90. doi: 10.1016/j.bbr.2012.12.052
- Ikegami, K., Shigeyoshi, Y., and Masubuchi, S. (2020). Circadian regulation of IOP rhythm by dual pathways of glucocorticoids and the sympathetic nervous system. *Invest. Ophthalmol. Visual Sci.* 61:26. doi: 10.1167/iovs.61.3.26
- Jiang, Y. H., Armstrong, D., Albrecht, U., Atkins, C. M., Noebels, J. L., Eichele, G., et al. (1998). Mutation of the Angelman ubiquitin ligase in mice causes increased cytoplasmic p53 and deficits of contextual learning and long-term potentiation. *Neuron* 21, 799–811. doi: 10.1016/s0896-6273(00)80596-6
- Jiang, Y. H., Pan, Y., Zhu, L., Landa, L., Yoo, J., Spencer, C., et al. (2010). Altered ultrasonic vocalization and impaired learning and memory in Angelman syndrome mouse model with a large maternal deletion from Ube3a to Gabrb3. *PLoS One* 5:e12278. doi: 10.1371/journal.pone.0012278
- Jones, K. A., Han, J. E., DeBruyne, J. P., and Philpot, B. D. (2016). Persistent neuronal Ube3a expression in the suprachiasmatic nucleus of Angelman syndrome model mice. *Sci. Rep.* 6, 1–13. doi: 10.1038/srep28238
- Judson, M. C., Sosa-Pagan, J. O., Del Cid, W. A., Han, J. E., and Philpot, B. D. (2014). Allelic specificity of Ube3a expression in the mouse brain during postnatal development. *J. Comp. Neurol.* 522, 1874–1896. doi: 10.1002/cne.23507
- Jung, M., and Lee, E. K. (2021). RNA-Binding Protein HuD as a versatile factor in neuronal and non-neuronal systems. *Biology* 10:361. doi: 10.3390/biology10050361
- Kim, A., Fujimoto, M., Hwa, V., Backeljauw, P., and Dauber, A. (2018). Adrenal insufficiency, sex reversal, and Angelman Syndrome due to uniparental disomy unmasking a mutation in CYP11A1. *Hormone Res. Paediat.* 89, 205–210. doi: 10.1159/000487638
- Krishnan, V., Stoppel, D. C., Nong, Y., Johnson, M. A., Nadler, M. J., Ozkaynak, E., et al. (2017). Autism gene Ube3a and seizures impair sociability by repressing VTA Cbln1. *Nature* 543, 507–512. doi: 10.1038/nature21678
- Laan, L. A., Haeringen, A., and Brouwer, O. F. (1999). Angelman syndrome: a review of clinical and genetic aspects. *Clin. Neurol. Neurosurg.* 101, 161–170.
- Le Minh, N., Damiola, F., Tronche, F., Schütz, G., and Schibler, U. (2001). Glucocorticoid hormones inhibit food-induced phase-shifting of peripheral circadian oscillators. *EMBO J.* 20, 7128–7136. doi: 10.1093/emboj/20.24.7128
- Lehman, N. L. (2009). The ubiquitin proteasome system in neuropathology. *Acta Neuropathol.* 118, 329–347. doi: 10.1007/s00401-009-0560-x
- Liska, K., Sladek, M., Houdek, P., Shrestha, N., Luzna, V., Ralph, M. R., et al. (2021). High sensitivity of circadian clock in the hippocampal dentate gyrus to glucocorticoid- and GSK3beta-dependent signals. *Neuroendocrinology.* 2021:689. doi: 10.1159/000517689
- Loffreda, A., Nizzardo, M., Arosio, A., Ruepp, M. D., Calogero, R. A., Volinia, S., et al. (2020). miR-129-5p: A key factor and therapeutic target in amyotrophic lateral sclerosis. *Prog. Neurobiol.* 190:101803. doi: 10.1016/j.pneurobio
- Morin, L. P., Hefton, S., and Studholme, K. M. (2011). Neurons identified by NeuN/Fox-3 immunoreactivity have a novel distribution in the hamster and mouse suprachiasmatic nucleus. *Brain Res.* 1421, 44–51. doi: 10.1016/j.brainres.2011.09.015
- Morris, E. L., Patton, A. P., Chesham, J. E., Crisp, A., Adamson, A., and Hastings, M. H. (2021). Single-cell transcriptomics of suprachiasmatic nuclei reveal a Prokineticin-driven circadian network. *EMBO J.* 6:e108614. doi: 10.15252/emboj.2021108614
- Nakao, M., Sutcliffe, J. S., Durtschi, B., Mutirangura, A., Ledbetter, D. H., and Beaudet, A. L. (1994). Imprinting analysis of three genes in the Prader-Willi/Angelman region: SNRPN, E6-associated protein, and PAR-2 (D15S225E). *Hum. Mol. Genet.* 3, 309–315. doi: 10.1093/hmg/3.2.309
- Okano, H. J., and Darnell, R. B. (1997). A hierarchy of Hu RNA binding proteins in developing and adult neurons. *J. Neurosci.* 17, 3024–3037. doi: 10.1523/JNEUROSCI.17-09-03024.1997
- Pelc, K., Cheron, G., Boyd, S. G., and Dan, B. (2008). Are there distinctive sleep problems in Angelman syndrome? *Sleep Med.* 9, 434–441. doi: 10.1016/j.sleep.2007.07.001
- Reppert, S. M., and Weaver, D. R. (2002). Coordination of circadian timing in mammals. *Nature* 418, 935–941. doi: 10.1038/nature00965
- Robb, S. A., Pohl, K. R., Baraitser, M., Wilson, J., and Brett, E. M. (1989). The 'happy puppet' syndrome of Angelman: review of the clinical features. *Arch. Dis. Childhood* 64, 83–86. doi: 10.1136/adc.64.1.83
- Rooszendaal, B. (2002). Stress and memory: opposing effects of glucocorticoids on memory consolidation and memory retrieval. *Neurobiol. Learn. Memory* 78, 578–595.
- Scammell, T. E., Arrigoni, E., and Lipton, J. O. (2017). Neural circuitry of wakefulness and sleep. *Neuron* 93, 747–765. doi: 10.1016/j.neuron.2017.01.014
- Schwartz, W. J., and Klerman, E. B. (2019). Circadian neurobiology and the physiologic regulation of sleep and wakefulness. *Neurol. Clin.* 37, 475–486. doi: 10.1016/j.ncl.2019.03.001
- Shi, S. Q., Bichell, T. J., Ihrle, R. A., and Johnson, C. H. (2015). Ube3a imprinting impairs circadian robustness in Angelman syndrome models. *Curr. Biol.* 25, 537–545. doi: 10.1016/j.cub.2014.12.047
- Shi, S. Q., and Johnson, C. H. (2019). Circadian biology and sleep in monogenic neurological disorders and its potential application in drug discovery. *Curr. Opin. Behav. Sci.* 25, 23–30. doi: 10.1016/j.cobeha.2018.06.006
- Sidorov, M. S., Deck, G. M., Dolatshahi, M., Thibert, R. L., Bird, L. M., Chu, C. J., et al. (2017). Delta rhythmicity is a reliable EEG biomarker in Angelman syndrome: a parallel mouse and human analysis. *J. Neurodevel. Disord.* 9:17. doi: 10.1186/s11689-017-9195-8
- Smith, A., Wiles, C., Haan, E., McGill, J., Wallace, G., Dixon, J., et al. (1996). Clinical features in 27 patients with Angelman syndrome resulting from DNA deletion. *J. Med. Genet.* 33, 107–112. doi: 10.1136/jmg.33.2.107
- Smith, S. E., Zhou, Y. D., Zhang, G., Jin, Z., Stoppel, D. C., and Anderson, M. P. (2011). Increased gene dosage of Ube3a results in autism traits and decreased glutamate synaptic transmission in mice. *Sci. Transl. Med.* 3:97. doi: 10.1126/scitranslmed.3002627
- Sonzogni, M., Wallaard, I., Santos, S. S., Kingma, J., du Mee, D., and van Woerden, G. M. (2018). A behavioral test battery for mouse models of Angelman syndrome: a powerful tool for testing drugs and novel Ube3a mutants. *Mol. Autism* 9, 1–19. doi: 10.1186/s13229-018-0231-7
- Sumová, A., Sládek, M., Jáè, M., and Illnerová, H. (2002). The circadian rhythm of Per1 gene product in the rat suprachiasmatic nucleus and its modulation by seasonal changes in daylength. *Brain Res.* 947, 260–270. doi: 10.1016/s0006-8993(02)02933-5
- Sutcliffe, J. S., Jiang, Y. H., Galijaard, R. J., Matsuura, T., Fang, P., Kubota, T. C., et al. (1997). The E6-AP ubiquitin-protein ligase (UBE3A) gene is localized within a narrowed Angelman syndrome critical region. *Genome Res.* 7, 368–377. doi: 10.1101/gr.7.4.368
- Takaesu, Y., Komada, Y., and Inoue, Y. (2012). Melatonin profile and its relation to circadian rhythm sleep disorders in Angelman syndrome patients. *Sleep Med.* 13, 1164–1170. doi: 10.1016/j.sleep.2012.06.015
- Thomas, A., Burant, A., Bui, N., Graham, D., Yuva-Paylor, L. A., and Paylor, R. (2009). Marble burying reflects a repetitive and perseverative behavior more than novelty-induced anxiety. *Psychopharmacology* 204, 361–373. doi: 10.1007/s00213-009-1466-y
- Trickett, J., Heald, M., and Oliver, C. (2017). Sleep in children with Angelman syndrome: parental concerns and priorities. *Res. Dev. Disabil.* 69, 105–115. doi: 10.1016/j.ridd.2017.07.017

- van Woerden, G. M., Harris, K. D., Hojjati, M. R., Gustin, R. M., Qiu, S., de Avila Freire, R., et al. (2007). Rescue of neurological deficits in a mouse model for Angelman syndrome by reduction of  $\alpha$ CaMKII inhibitory phosphorylation. *Nature Neurosci.* 10, 280–282. doi: 10.1038/nn1845
- Weeber, E. J., Jiang, Y. H., Elgersma, Y., Varga, A. W., Carrasquillo, Y., Brown, S. E., et al. (2003). Derangements of hippocampal calcium/calmodulin-dependent protein kinase II in a mouse model for Angelman mental retardation syndrome. *J. Neurosci.* 23, 2634–2644. doi: 10.1523/JNEUROSCI.23-07-02634.2003
- Wen, S., Ma, D., Zhao, M., Xie, L., Wu, Q., Gou, L., et al. (2020). Spatiotemporal single-cell analysis of gene expression in the mouse suprachiasmatic nucleus. *Nature Neurosci.* 23, 456–467. doi: 10.1038/s41593-020-0586-x
- Williams, C. A., Beaudet, A. L., Clayton-Williams, C. A., Beaudet, A. L., Clayton-Smith, J., Knoll, J. H., et al. (2006). Angelman syndrome 2005: updated consensus for diagnostic criteria. *Am. J. Med. Genet. Part A* 140, 413–418. doi: 10.1002/ajmg.a.31074
- Xu, P., Berto, S., Kulkarni, A., Jeong, B., Joseph, C., Cox, K. H., et al. (2021). NPAS4 regulates the transcriptional response of the suprachiasmatic nucleus to light and circadian behavior. *Neuron*. 109, 3268–3282. doi: 10.1016/j.neuron.2021.07.026
- Yamasaki, K., Joh, K., Ohta, T., Masuzaki, H., Ishimaru, T., Mukai, T., et al. (2003). Neurons but not glial cells show reciprocal imprinting of sense and antisense transcripts of *Ube3a*. *Human Mol. Genet.* 12, 837–847. doi: 10.1093/hmg/ddg106
- Yoo, S. H., Yamazaki, S., Lowrey, P. L., Shimomura, K., Ko, C. H., Buhr, E. D., et al. (2004). PERIOD2::LUCIFERASE real-time reporting of circadian dynamics reveals persistent circadian oscillations in mouse peripheral tissues. *Proc. Nat. Acad. Sci.* 101, 5339–5346. doi: 10.1073/pnas.0308709101

**Conflict of Interest:** AB was employed by Luna Genetics, Inc.

The remaining authors declare that the research was conducted in the absence of any commercial or financial relationships that could be construed as a potential conflict of interest.

**Publisher's Note:** All claims expressed in this article are solely those of the authors and do not necessarily represent those of their affiliated organizations, or those of the publisher, the editors and the reviewers. Any product that may be evaluated in this article, or claim that may be made by its manufacturer, is not guaranteed or endorsed by the publisher.

Copyright © 2022 Shi, Mahoney, Houdek, Zhao, Anderson, Zhuo, Beaudet, Sumova, Scammell and Johnson. This is an open-access article distributed under the terms of the Creative Commons Attribution License (CC BY). The use, distribution or reproduction in other forums is permitted, provided the original author(s) and the copyright owner(s) are credited and that the original publication in this journal is cited, in accordance with accepted academic practice. No use, distribution or reproduction is permitted which does not comply with these terms.